

Spatial Confinement of Laser Light in Active Random Media

H. Cao, J. Y. Xu, and D. Z. Zhang

Department of Physics and Astronomy, Materials Research Center, Northwestern University, Evanston, Illinois 60208

S.-H. Chang and S. T. Ho

Department of Electrical and Computer Engineering, Materials Research Center, Northwestern University, Evanston, Illinois 60208

E. W. Seelig, X. Liu, and R. P. H. Chang

Department of Materials Science and Engineering, Materials Research Center, Northwestern University, Evanston, Illinois 60208

(Received 9 December 1999)

We have observed spatial confinement of laser light in micrometer-sized random media. The optical confinement is attributed to the disorder-induced scattering and interference. Our experimental data suggest that coherent amplification of the scattered light enhances the interference effect and helps the spatial confinement. Using the finite-difference time-domain method, we simulate lasing with coherent feedback in the active random medium.

PACS numbers: 71.55.Jv, 42.25.Fx

In a random medium, optical scattering may induce a phase transition in the photon transport behavior [1]. When the scattering is weak, the propagation of light can be described by a normal diffusion process. With an increase in the amount of scattering, recurrent light scattering events arise. Interference between the counterpropagating waves in a disordered structure gives rise to the enhanced backscattering, also called weak localization [2,3]. When the amount of scattering is increased beyond a critical value, the system makes a transition into a localized state. Light propagation is inhibited due to the interference in multiple scattering [4–7]. Theoretically, a localized state is an eigenstate of an infinitely large random medium. When the medium size is finite, light leakage from the edges of the medium results in a finite lifetime of the localized state, and thereby a width $\delta\nu$ of its energy level. The Thouless number $\delta \equiv \delta\nu/(d\nu/dN)$, where $d\nu/dN$ is the level spacing. Anderson localization threshold is given by the Thouless criterion, $\delta = 1$ [8,9].

It is well known that optical absorption destroys photon localization because it suppresses the interference of scattered light. Optical gain, which has the opposite effect of absorption, should enhance photon localization. In the case of weak localization, the amplification of the backscattered light narrows the enhanced backscattering peak [10]. For a one-dimensional random medium, photon localization length is reduced in the presence of gain due to the amplification of the coherent backscattering effect [11]. Recently, we demonstrated that recurrent light scattering can provide coherent feedback for lasing in a three-dimensional random medium [12]. In this Letter, we have further enhanced the scattering strength in zinc oxide (ZnO) powder by reducing the particle size, and observed spatial confinement of laser light in the disordered medium.

ZnO nanoparticles are synthesized with the precipitation reaction. The process involves hydrolysis of zinc salt in a polyol medium. Through the process of electrophoresis,

ZnO powder films are made. The film thickness is about $30\ \mu\text{m}$. According to the scanning electron microscope (SEM) image of the ZnO particles, the average particle size is about 50 nm. The scattering mean free path l in the ZnO powder is characterized in the coherent backscattering experiment [2,3]. To avoid absorption, the probe photon energy is slightly less than the ZnO band gap energy (3.3 eV). From the angular width of the backscattering cone, we estimate $l \sim 0.5\lambda$.

In the photoluminescence experiment, the ZnO powder film is optically pumped by the fourth harmonics ($\lambda = 266\ \text{nm}$) of a mode-locked Nd:YAG laser (10 Hz repetition rate, 20 ps pulse width). The pump beam is focused to a $\sim 20\ \mu\text{m}$ spot on the film surface with normal incidence. The spectrum of emission from the powder film is measured by a spectrometer with 0.13 nm spectral resolution. At the same time, the spatial distribution of the emitted light intensity in the film is imaged by an ultraviolet (UV) microscope onto a UV sensitive charge-coupled device (CCD) camera. The amplification of the microscope is about 100 times. The spatial resolution is around $0.24\ \mu\text{m}$. A bandpass filter is placed in front of the microscope objective to block the pump light.

Figure 1 shows the measured spectra and spatial distribution of emission in a ZnO powder film at different pump power. At low pump intensity, the spectrum consists of a single broad spontaneous emission peak. Its full width at half maximum (FWHM) is about 12 nm [Fig. 1(a)]. In Fig. 1(b), the spatial distribution of the spontaneous emission intensity is smooth across the excitation area. Because of the pump intensity variation over the excitation spot, the spontaneous emission in the center of the excitation spot is stronger. When the pump intensity exceeds a threshold, sharp peaks emerge in the emission spectrum [Fig. 1(c)]. The FWHM of these peaks is about 0.2 nm. Simultaneously, bright tiny spots appear in the image of the emitted light distribution in the film [Fig. 1(d)]. The

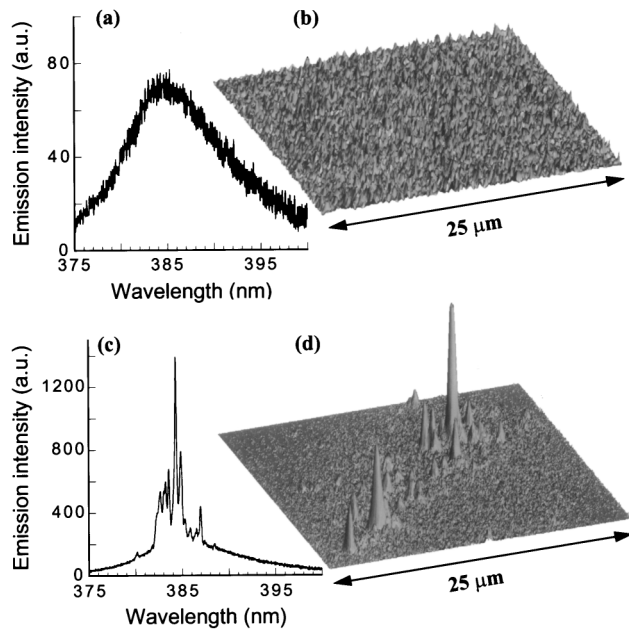


FIG. 1. (a) and (c) are the measured spectra of emission from the ZnO powder film. (b) and (d) are the measured spatial distribution of emission intensity in the film. The incident pump pulse energy is 5.2 nJ for (a) and (b), and 12.5 nJ for (c) and (d).

size of the bright spots is between 0.3 and 0.7 μm . When the pump intensity is increased further, additional sharp peaks emerge in the emission spectrum. Correspondingly, more bright spots appear in the image of the emitted light distribution. Above the threshold, the total emission intensity increases much more rapidly with the pump power. Hence, laser action has occurred in the powder film.

The experimental fact that the bright spots in the emission pattern and the lasing modes in the emission spectrum always appear simultaneously suggests that the bright spots are related to the laser light. There seem to be two possible explanations for the bright spots. One is that the laser light intensity at the locations of the bright spots is high. The other is that the laser light is not particularly strong at the locations of the bright spots. However, there are some efficient scattering centers at the locations of the bright spots, and thus the laser light is strongly scattered. In the latter case, these scattering centers should also strongly scatter the spontaneously emitted light below the lasing threshold, because scattering is a linear process. Hence, these bright spots should exist below the lasing threshold. However, there are no bright spots below the lasing threshold. Therefore, these bright spots are caused not by efficient scatterers, but by strong laser light in the medium.

Next we present an explanation for our experimental data. The short scattering mean free path indicates very strong light scattering in the powder film. However, the scattering mean free path obtained from the coherent back-scattering measurement is an average over a large volume of the sample. Because of the local variation of particle density and spatial distribution, there exist small regions

of higher disorder and stronger scattering. Light can be confined in these regions through multiple scattering and interference. For a particular configuration of scatterers, only light at certain wavelengths can be confined, because the interference effect is wavelength sensitive. In a different region of the sample, the configuration of the scatterers is different, and thus light at different wavelengths is confined. In other words, there are many resonant cavities formed by multiple scattering and interference. When the optical gain reaches the loss of a cavity, laser oscillation occurs. The lasing peaks in the emission spectrum illustrate the cavity resonant frequencies, and the bright spots in the spatial light pattern exhibit the positions and shapes of the cavities.

To check the above explanation, we have reduced the size of the random medium to approximately the size of an intense laser radiation region in the powder film by agglomerating ZnO nanoparticles to form clusters [13]. Indeed, we have achieved lasing in micrometer-sized ZnO clusters. The inset of Fig. 2 is the SEM image of a ZnO cluster. Its size is slightly larger than 1 μm , and it contains roughly 20 000 particles. The pump light is focused by a UV microscope objective onto the cluster. Figure 2 plots the spectrally integrated intensity of emission from the cluster as a function of the incident pump pulse energy. A threshold behavior is clearly seen. The incident pump pulse energy required to reach the lasing threshold is around 0.2 nJ. Below the lasing threshold, the emission spectrum consists of a single broad spontaneous emission peak. The spatial distribution of the spontaneous emission intensity is uniform across the cluster. Above the lasing threshold, a sharp peak emerges in the emission spectrum [Fig. 3(a)]. Its FWHM is 0.16 nm. After taking

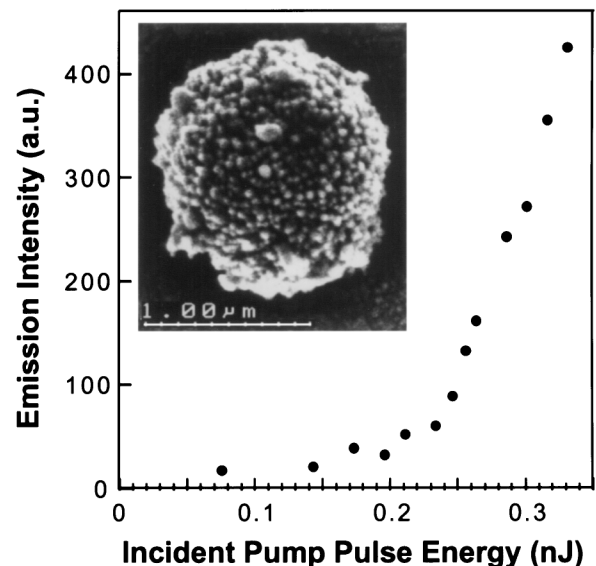


FIG. 2. Spectrally integrated intensity of emission from the ZnO cluster as a function of the incident pump pulse energy. The inset is the SEM image of the cluster.

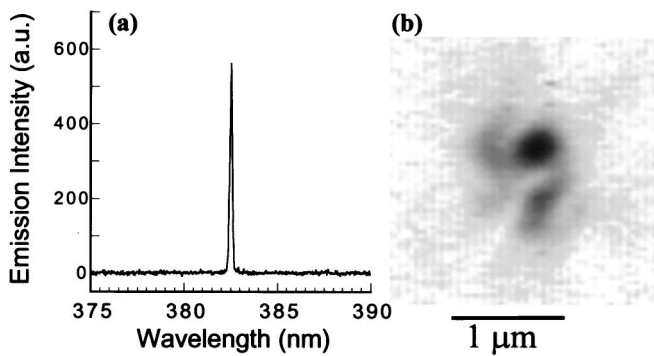


FIG. 3. (a) The measured spectra of emission from the ZnO cluster. (b) The measured spatial distribution of emission intensity in the cluster. The incident pump pulse energy is 0.25 nJ.

into account the instrumental broadening, the actual width of the peak is only 0.09 nm. Simultaneously, a couple of bright spots appear in the image of laser light distribution across the cluster [Fig. 3(b)]. By adjusting the microscope objective, light distribution on different planes inside the cluster is imaged onto the CCD camera. We find the emission pattern on different planes inside the cluster consists of different bright spots. This suggests that the bright spots are buried with different depth inside the cluster. The spatial distribution of the laser light intensity exhibits the spatial profile of the lasing mode. When the pump power is increased further, a second lasing mode emerges in the emission spectrum. Correspondingly, additional bright spots appear in the image of the emitted light distribution.

Because of a large number of defects in the ZnO particles, the nonradiative recombination of the excited carriers is significant below the lasing threshold. The lifetime of the excited carriers is about 200 ps. Above the lasing threshold, since the stimulated emission process is very fast (less than 50 ps), the radiative recombination of the excited carriers becomes dominant, leading to a rapid increase of the total emission intensity (Fig. 2).

Several models have been set up in the theoretical study of the stimulated emission in an active random medium, e.g., the diffusion equation with gain [14,15], the Monte Carlo simulation [16], and the ring laser with nonresonant feedback [17]. However, these models cannot predict lasing with coherent feedback because the phase of the optical field is neglected. We take a different approach: namely, we directly calculate the electromagnetic field distribution in a random medium by solving the Maxwell equations using the finite-difference time-domain (FDTD) method [18]. The advantage of this approach is that we can model the real structure of a disordered medium, and calculate both the emission pattern and the emission spectrum.

In our model, ZnO particles are randomly positioned in space. The particle size is 50 nm. The random medium has a finite size, and it is surrounded by air. To model the situation that the random medium is located in infinitely large space, we use the uniaxial perfectly matched layer

(UPML) absorbing boundary condition to absorb all the outgoing light wave in the air [19]. We solve the Maxwell curl equations in the time domain after introducing optical gain by the negative conductance σ [20]. The randomness is introduced to the Maxwell equations through the dielectric constant ϵ , which varies spatially due to the random distribution of the ZnO particles. The refractive index of ZnO is about 2.3.

In our simulation, a seed pulse, whose spectrum covers the ZnO emission spectrum, is launched in the center of the random medium at $t = 0$. When the optical gain is above the lasing threshold, the electromagnetic field oscillation builds up in the time domain. Using the discrete Fourier transform of the time domain data, we obtain the emission spectrum. Figure 4 shows the calculated emission spectrum and emission pattern for a specific configuration of scatterers. The size of the random medium is 3.2 μm . The filling factor of ZnO particles is 0.5. When the optical gain is just above the lasing threshold, the emission spectrum, shown in Fig. 4(a), consists of a single peak. Figure 4(b) represents the light intensity distribution in the random medium. There are a few bright spots near the center. At the edge of the random medium, the light intensity is almost zero. To check the effect of the boundary, we change the spatial distribution of the scatterers near the edges of the random medium. We find both the emission frequency and the emission pattern remain the same. Their independence of the boundary condition indicates that the lasing mode is formed by multiple scattering and interference inside the disordered medium. When the optical gain is increased further, additional lasing mode appears.

We conclude with some comment. Our experimental data suggest that optical gain helps spatial confinement of light in a random medium. The uniform distribution of spontaneous emission intensity across the excitation area in Fig. 2(b) indicates that the pump light is not spatially confined in small regions in the medium. Otherwise, the spontaneous emission from these regions with high pump intensity would be much stronger than that from other regions. We believe this is because the pump light experiences strong absorption which suppresses the interference of the scattered light. Furthermore, the emission patterns in the ZnO powder films and the ZnO clusters illustrate

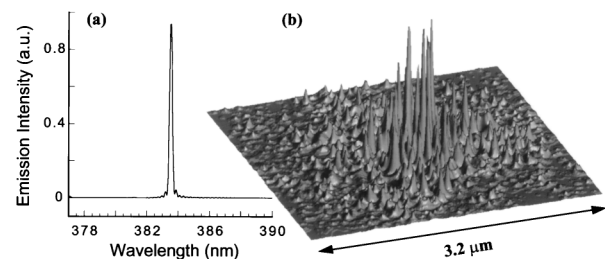


FIG. 4. (a) The calculated emission spectrum. (b) The calculated spatial distribution of emission intensity in the random medium.

that the emitted light is not spatially confined at low pump power, but at high pump power it is spatially confined. This phenomenon suggests that coherent amplification of the scattered emission (with the persistence of phase coherence) enhances the interference effect and leads to spatial confinement of the emitted light.

What is the relation of the spatial confinement of laser light in an active random medium to the Anderson localization of light? The SEM images reveal that there is no local order in the ZnO powder. The spatial confinement of laser light in the ZnO powder results from disorder-induced scattering and interference. Anderson localization of light is based on the same mechanism. However, all the study of Anderson localization is conducted on passive random media. There is no criterion for Anderson localization in an active random medium. If we extend the Thouless criterion for Anderson localization to an active random medium, we can calculate the Thouless number above the lasing threshold. For the ZnO cluster shown in Fig. 2, the level spacing $d\nu/dN = c\lambda^2/8\pi n^3V = 2.4 \times 10^{11}$ Hz, where n is the effective index of refraction, and V is the volume of the cluster. The linewidth of the lasing mode in Fig. 3 is $\delta\nu = 1.8 \times 10^{11}$ Hz. Hence, the Thouless number $\delta = 0.75 < 1$. This seems to suggest that Anderson localization occurs at the lasing mode.

This work is supported partially by the National Science Foundation under Grant No. ECS-9877113, and by the NSF MRSEC program (No. DMR-9632472) at the Materials Research Center of Northwestern University. H. C. acknowledges support from the David and Lucile Packard Foundation.

[1] S. John, Phys. Today **32**, No. 5, 32 (1991).

- [2] M.P. van Albada and A. Lagendijk, Phys. Rev. Lett. **55**, 2692 (1985).
- [3] P.E. Wolf and G. Maret, Phys. Rev. Lett. **55**, 2696 (1985).
- [4] A.Z. Genack and N. Garcia, Phys. Rev. Lett. **66**, 2064 (1991).
- [5] R. Dalichaouch, J.P. Armstrong, S. Schultz, P.M. Platzman, and S.L. McCall, Nature (London) **354**, 53 (1991).
- [6] D.S. Wiersma, P. Bartolini, A. Lagendijk, and R. Righini, Nature (London) **390**, 671 (1997).
- [7] F.J.P. Schuurmans, D. Vanmaekelbergh, J. van de Lage-maat, and A. Lagendijk, Science **284**, 141 (1999).
- [8] E. Abrahams, P.W. Anderson, D.C. Licciardello, and T.V. Ramakrishnan, Phys. Rev. Lett. **42**, 673 (1979).
- [9] D.J. Thouless, Phys. Rev. Lett. **39**, 1167 (1977).
- [10] D.S. Wiersma, M.P. Van Albada, and A. Lagendijk, Phys. Rev. Lett. **75**, 1739 (1995).
- [11] Z.-Q. Zhang, Phys. Rev. B **52**, 7960 (1995).
- [12] H. Cao, Y.G. Zhao, S.T. Ho, E.W. Seelig, Q.H. Wang, and R.P.H. Chang, Phys. Rev. Lett. **82**, 2278 (1999).
- [13] D. Jezequel, J. Guenot, N. Jouini, and F. Fievet, J. Mater. Res. **10**, 77 (1995).
- [14] D.S. Wiersma and A. Lagendijk, Phys. Rev. E **54**, 4256 (1996).
- [15] S. John and G. Pang, Phys. Rev. A **54**, 3642 (1996).
- [16] G.A. Berger, M. Kempe, and A.Z. Genack, Phys. Rev. E **56**, 6118 (1997).
- [17] R.M. Balachandran and N.M. Lawandy, Opt. Lett. **22**, 319 (1997).
- [18] A. Taflove, *Computational Electrodynamics: The Finite-Difference Time-Domain Method* (Artech House, Boston, 1995).
- [19] Z.S. Sacks, D.M. Kingsland, R. Lee, and J.F. Lee, IEEE Trans. Antennas Propag. **43**, 1460 (1995).
- [20] S.C. Hagness, R.M. Joseph, and A. Taflove, Radio Sci. **31**, 931 (1996).